RPE | Radiation Physics & Engineering
A Peer-Reviewed Journal
Published by K.N. Toosi University of Technology
http://rpe.kntu.ac.ir
Research Article

Radiation Physics and Engineering 2023; 4(2):53–60

Assignment of a radiological map of the city of Borujerd in Iran

Reza Pourimani*, Mobin Bajelan, Monire Mohebian
Department of Physics, Faculty of Science, Arak University, Arak, Iran

HIGHLIGHTS

- Measurement of natural radionuclides in soil samples of Borujerd city.
- Calculation of radiometric parameters for these samples.
- Comparison of them contains with other reported work from other countries.
- Provided discussion about of radiological indices.
- Drown radiological map of Borujerd city.

ABSTRACT

The specific activity of radionuclides in the soil of the Borujerd region using high purity Germanium detector (HPGe) was measured and the associated radiological hazards were calculated. The mean specific activity of radionuclides of Ra-226, Th-232, K-40, and Cs-137 in soil was obtained at 10.99 ± 5.11, 35.36 ± 4.44, 324.20 ± 10.24, and 2.93 ± 0.60 Bq.kg^{-1}. These values were below the global average. Also, the value of basic radiological risk parameters, such as Ra_{eq}, AED_{out}, AED_{int}, H_{ex}, H_{in}, and I_{γ}, ranged from 52.02 to 139.54 in Bq.kg^{-1}, from 24.98 to 68.27 and from 42.90 to 117.22 in mSv.y^{-1}, 122.57 to 334.93, 0.14 to 0.37, 0.16 to 0.40, and 0.27 to 1.04, respectively. The range of excess lifetime cancer risk (ELCR) value for the surrounding soil samples varied from 0.15×10^{-3} to 0.41×10^{-3}, in which samples S4, S14, S24, S27, S28, S29, and S30 exceeded the global average of 0.29×10^{-3}. A radiological map of the city of Borujerd was prepared using the GIS program. The study showed that the level of radioactivity in the Borujerd area did not exceed the critical value and is in line with the global results.

KEYWORDS

Radionuclide
Radiological map
Radiological indices
HPGe

HISTORY

Received: 13 November 2022
Revised: 7 December 2022
Accepted: 22 December 2022
Published: Spring 2023

1 Introduction

Humans are always affected by nuclear radiation from naturally occurring radioactive nuclei such as elements in the U-238 and Th-232 chains and some radioactive nuclei such as radionuclide K-40. The high level of potassium in the soil is due to the fact that it makes up an average of 2.8% of soil weight. On average, the amount of uranium and thorium in soil was estimated as 2.7 and 9.6 mg.kg^{-1} (Mohebian and Pourimani, 2019). In addition to natural radiation, our environment also has radiation induced by special artificial radioactive nuclei, such as Cs-137 and Sr-90 (UNSCEAR, 2000). Cs-137 is one of the fission products created and released into the environment due to nuclear accidents such as the explosion of the Chernobyl reactor in Ukraine (1986) (UNSCEAR, 2000).

Due to the harmful nature of nuclear radiation to human health, it is necessary to conduct soil monitoring in areas where people live and are exposed to natural and artificial nuclear radiation. This is important for determining the distribution and radiological mapping of radionuclides in residential and food-producing regions. In the field of measuring the amount of radioactivity in soil samples, countless types of research have been conducted in the countries of Iraq, Turkey, Saudi Arabia, Pakistan, India, Congo, China, Egypt, Malaysia, and also in Iran (Agbalagba and Onoja, 2011; Hussain and Alzhraa, 2017; Adewoyin et al., 2022; Hasan and Majeed, 2013; Dizman et al., 2016; Alshahri and El-Taher, 2019; Khan et al., 2020; Suresh et al., 2020; Diahou et al., 2022; Ziqiang et al., 1988; El-Araby et al., 2021; Alzubaidi et al., 2016; Pourimani et al., 2017; Mohebian and Pourimani, 2020). This study specifies the distribution of radionuclides and a radiological map of the city of Borujerd in the central region of Iran.

*Corresponding author: r-pourimani@araku.ac.ir

https://doi.org/10.22034/rpe.2022.370078.1108
https://dorl.net/dor/20.1001.1.26456397.2023.4.2.7.3

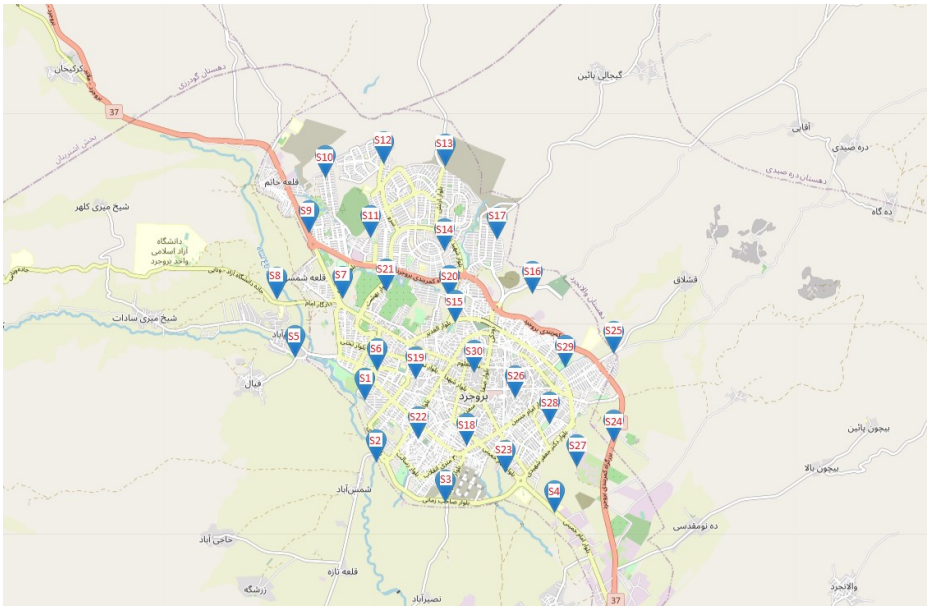

Figure 1: Sampling points area of Borujerd city in Iran.

2 Materials and Methods

2.1 Area and sampling method

In the present study, 30 soil samples were taken from surface soils (less than 10 cm depth) in the Borujerd areas of Iran, and the longitude and latitude of the sampling site were recorded with the Global Positioning System (GPS). Figure 1 shows the sampling area that covered the entire city area.

2.2 Preparation of samples

500 g of soil were collected from the sampling points and transported in a plastic bag with a region label. In accordance with the International Atomic Energy Organization's environmental sample preparation and packaging instructions, 300 g of powder after grinding and passing the samples through 20 and 50 mesh was packed, sealed, and encoded in cylindrical containers of 300 g (Barnett et al., 2009). Coding was done according to the geographical location of each sample. Soil samples were sealed with silicon glue. The seal of the container prevents the release of radon gas in the uranium chain. To measure the amount of Ra-226, it is necessary to establish a secular equilibrium between radium and radon so that the sample containers are tightly closed for at least 50 days before the measurement (Jibiri and Esen, 2011). In the event of the release of radon gas, the activity of the radium nucleus cannot be obtained from the activity of the radon daughter nuclei (Ranjbar and Yousefi, 2019).

2.3 Radionuclide analysis of samples

To determine the specific activities of radionuclides in the samples, it is necessary to calibrate the energy and efficiency of the detector-sample system. Energy and efficiency calibration was done using a standard RGU-1 and Cs-137 sources of known activity (Pourimani and Davood Maghami, 2020). RGU-1 is a known reference material in the form of a fine powder with known activity that can be used in any configuration, including a sample container. The relationship between energy and channel is shown in Eq. (1):

$$Energy = 7.52 + (0.33 \times Channel) \tag{1}$$

High purity germanium detector system was used in this research. The GCD30195BSI model detector operated at voltage of 3000 V, an energy resolution of 1.95 keV and a relative efficiency of 30%. The gamma ray spectrum of each sample was registered using LSRMBSI software. The spectra were analyzed using Gamma Vision Master II Ortec EG software. The efficiency value of gamma lines was determined using Eq. (2) (Hossain et al., 2010):

$$\epsilon(\%) = \frac{Net\ Area}{A \times BR(\%) \times T} \times 100 \tag{2}$$

where NetArea is the net count under the full energy peak corresponding to the energy E_i, A is the specific activity of the radionuclide, BR (%) is the probability of E_i photon emission, and T specifies the counting time. The graph of efficiency as a function of gamma-ray energy plotted using the Matlab program is shown in Fig. 2. The gamma ray spectrum of each sample was recorded for 86,400 s. Background radiation was measured with an empty container under the same conditions and subtracted from each spectrum (Pourimani and Mohebian, 2021).

2.3.1 Measuring the specific activity of radioactive nuclei

Using the net count under full peak energy ($NetArea$), detector-sample efficiency (ϵ), sample weight (m), and gamma emission probability (BR), the specific activities of Ra-226, Th-232, K-40, and Cs-137 in the samples were

calculated using Eq. (3) (Kabir et al., 2009):

$$A = \frac{Net\ Area}{\epsilon(\%) \times BR(\%) \times T \times m} \times 100 \quad (3)$$

So that A is the specific activity of the radionuclide in the sample in Bq.kg^{-1}, T is the counting time in seconds. The global average value of the specific activity of radium, thorium and potassium nuclei is 30, 35, and 412 Bq.kg^{-1} (Annex et al., 2000). The activity of Ra-226 was calculated from the gamma emission of Pb-214 (351.93 keV) and Bi-214 (609.31 keV). Th-232 activity was determined using gamma energies of Pb-212 (238.6 keV), Ac-228 (911.21 and 968.97 keV), and Tl-208 (583.2 keV). The K-40 activity was assessed directly with its gamma radiation (1460.75 keV) and Cs-137 activity was determined using its gamma line as 661.66 keV.

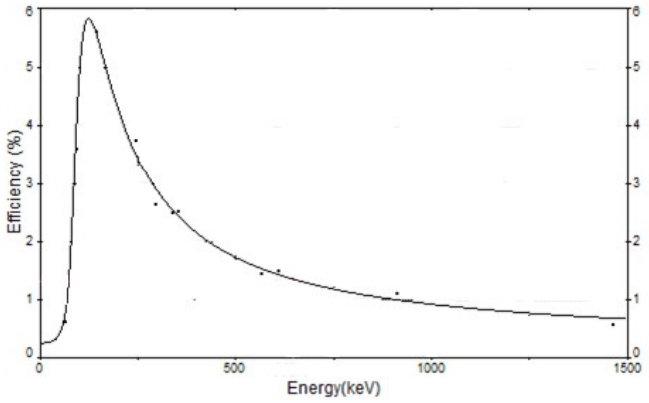

Figure 2: Efficiency diagram of the detector-sample configuration as a function of gamma-ray energy.

2.3.2 Radium equivalent activity

Ra equivalent activity is a single quantity that is used to determine the radiation level of natural radionuclides in terms of Ra-226 radioactivity and is one of the most common indicators of radiation level. This indicator is based on the evaluation that 370 Bq.kg^{-1} of Ra-226, 259 Bq.kg^{-1} of Th-232, and 4180 Bq.kg^{-1} of K-40 give the same gamma dose rate. It can be calculated using Eq. (4) (UNSCEAR, 2000):

$$Ra_{eq} = A_{\mathrm{Ra}} + 1.43A_{\mathrm{Th}} + 0.077A_{\mathrm{K}} \quad (4)$$

2.3.3 The absorbed dose rate in the air

At a height of 1 m above the ground, for radionuclides uniformly distributed in soil and rock, the absorbed gamma radiation dose (D) in the air can be calculated using Eq. (5) (UNSCEAR, 2000):

$$D\ (\mathrm{nGy.h^{-1}}) = 0.427\,A_{\mathrm{Ra}} + 0.662\,A_{\mathrm{Th}} + 0.0432\,A_{\mathrm{K}} \quad (5)$$

2.3.4 Internal and external annual effective dose

The annual effective dose in open air (AED) in terms of μSv.y^{-1} is related to the dose absorbed in the air (D) at a height of 1 m from the soil surface in terms of nGy.h^{-1} (Eqs. (6) and (7)). Since soil sampling is possible in materials, if a building is used, the annual effective dose inside the building has also been calculated (Pourimani and Mohebian, 2021).

$$AED_{outdoor}\ (\mu\mathrm{Sv.y^{-1}}) = Dose\ rate\ (\mathrm{nGy.h^{-1}}) \times 8760\ (\mathrm{h.y^{-1}}) \times 0.20 \times 0.7\ (\mathrm{Sv.Gy^{-1}}) \times 10^{-3} \quad (6)$$

$$AED_{indoor}\ (\mu\mathrm{Sv.y^{-1}}) = Dose\ rate\ (\mathrm{nGy.h^{-1}}) \times 8760\ (\mathrm{h.y^{-1}}) \times 0.8 \times 0.7\ (\mathrm{Sv.Gy^{-1}}) \times 10^{-3} \quad (7)$$

The internal and external occupancy factors are 0.80 and 0.20 respectively, and also a factor of 0.7 was used for the Gy to Sv conversion (Pourimani and Mohebian, 2021).

2.3.5 Calculation of internal and external risk indicators

The external risk index shows the amount of gamma radiation in the environment and the presence of radioactive nuclei in soils and rocks that may pose a threat to humans. The internal risk index is caused by inhalation of radon gas or ingestion of radionuclides. These parameters are calculated using Eqs. (8) and (9) (Kabir et al., 2009). For a safe environment, the maximum values of external and internal radiation risk indicators should be less than 1 (UNSCEAR, 2000).

$$H_{ex} = \frac{A_{\mathrm{Ra}}}{370} + \frac{A_{\mathrm{Th}}}{259} + \frac{A_{\mathrm{K}}}{4810} \leq 1 \quad (8)$$

$$H_{in} = \frac{A_{\mathrm{Ra}}}{185} + \frac{A_{\mathrm{Th}}}{259} + \frac{A_{\mathrm{K}}}{4810} \leq 1 \quad (9)$$

2.3.6 Calculation of gamma index (I_γ)

The gamma index is used to estimate the level of exposure to gamma radiation associated with naturally occurring radionuclides in soil and rocks. Equation (10) is used to calculate this index (Annex et al., 2000):

$$I_\gamma = \frac{A_{\mathrm{Ra}}}{150} + \frac{A_{\mathrm{Th}}}{100} + \frac{A_{\mathrm{K}}}{1500} \quad (10)$$

In Eqs. (4) to (10), A_{Ra}, A_{Th}, and A_{K} are the specific activities of Ra-226, Th-232, and K-40 in Bq.kg^{-1}, respectively.

2.3.7 Excess Lifetime Cancer Risk

The Excess Lifetime Cancer Risk ($ELCR$) is proportional to the absorbed annual effective dose (AED), life expectancy (LE), and risk factor (RF). Equation (11) using for the calculation of this important index. The Excess Lifetime Cancer Risk during the lifetime causes by environmental gamma radiation (UNSCEAR, 2000).

According to the World Health Organization report for Iranians, LE was 73.15 years (ÇINAR and Altundaş,

Table 1: The specific activities of natural radionuclides, Cs-137, radium equivalent, and absorbed dose rate in the air. MDA shows th Minimum Detectable Activity.

Sample code	Specific activity (Bq.kg^{-1})				Radiological Index	
	Ra-226	Th-232	K-40	Cs-137	Ra_{eq} (Bq.kg^{-1})	D (nG.h^{-1})
S1	17.63 ± 0.78	23.00 ± 3.78	363.85 ± 9.84	0.36 < MDA	78.53	38.47
S2	10.40 ± 0.89	67.10 ± 5.57	376.24 ± 10.48	1.11 < MDA	135.32	65.11
S3	6.16 ± 0.84	33.90 ± 4.53	513.85 ± 12.12	0.93 < MDA	94.20	47.27
S4	7.11 ± 0.85	40.80 ± 4.83	516.98 ± 12.34	1.04 < MDA	105.26	52.37
S5	2.56 ± 0.76	27.41 ± 4.13	380.56 ± 9.71	0.96 < MDA	71.05	35.67
S6	3.73 ± 0.77	45.77 ± 4.65	407.13 ± 10.07	0.94 < MDA	100.53	49.48
S7	29.85 ± 2.14	25.41 ± 3.77	293.26 ± 8.21	3.49 ± 0.32	87.76	42.23
S8	9.72 ± 0.69	31.40 ± 4.16	315.56 ± 9.02	0.90 < MDA	78.92	38.56
S9	2.39 ± 0.75	31.58 ± 4.04	353.58 ± 9.35	0.94 < MDA	75.31	37.20
S10	MDA > 2.61	41.74 ± 4.51	265.20 ± 7.58	0.89 < MDA	80.10	39.08
S11	2.58 ± 0.72	22.46 ± 3.80	306.69 ± 8.51	0.85 < MDA	58.31	29.21
S12	MDA > 2.56	41.41 ± 4.76	490.91 ± 12.05	0.96 < MDA	97.01	48.62
S13	26.74 ± 2.02	17.06 ± 3.59	228.46 ± 7.22	0.84 < MDA	68.72	32.58
S14	8.96 ± 0.83	42.57 ± 4.80	487.42 ± 12.68	0.99 < MDA	107.36	53.06
S15	5.25 ± 0.78	33.20 ± 4.53	252.02 ± 8.88	0.93 < MDA	72.13	35.10
S16	29.66 ± 2.19	17.88 ± 3.99	159.01 ± 6.72	1.25+0.30	67.47	31.37
S17	8.13 ± 0.73	32.55 ± 3.88	280.51 ± 9.11	0.93 < MDA	76.27	37.13
S18	7.01 ± 0.81	35.24 ± 4.53	252.98 ± 9.36	0.97 < MDA	76.88	37.25
S19	5.70 ± 0.80	36.04 ± 4.42	261.48 ± 9.36	0.99 < MDA	77.37	37.58
S20	12.33 ± 0.68	23.25 ± 5.02	226.23 ± 8.02	0.92 < MDA	65.71	30.42
S21	11.48 ± 0.69	18.99 ± 3.84	173.92 ± 8.03	0.94 < MDA	52.02	24.98
S22	14.48 ± 0.74	20.11 ± 4.57	191.35 ± 8.79	0.97 < MDA	57.97	27.76
S23	23.50 ± 0.84	27.61 ± 4.83	351.50 ± 10.29	1.01 < MDA	90.04	43.49
S24	13.48 ± 0.67	40.54 ± 6.05	458.51 ± 11.75	4.45 ± 0.40	106.75	52.40
S25	6.10 ± 0.70	34.78 ± 4.04	413.57 ± 9.90	3.33+0.30	87.68	43.49
S26	7.84 ± 0.71	40.77 ± 4.33	427.40 ± 10.15	2.15 ± 0.28	99.05	48.20
S27	6.42 ± 0.74	47.09 ± 4.27	539.22 ± 12.21	0.94 < MDA	115.27	57.20
S28	10.19 ± 0.79	53.15 ± 4.77	505.13+11.8	0.97 < MDA	125.08	61.35
S29	9.74+0.78	62.10 ± 4.94	532.55 ± 12.29	0.97 < MDA	139.54	68.27
S30	8.57 ± 0.74	45.87 ± 4.43	488.46 ± 11.45	0.92 < MDA	111.77	55.12
MIN	MDA > 2.56	17.06 ± 3.59	159.01 ± 6.72	0.36 < MDA	52.02	24.98
MAX	29.845 ± 2.14	67.10 ± 5.57	539.22 ± 12.21	4.45 ± 0.40	139.54	68.27
MEAN	10.99 ± 5.11	35.36 ± 4.44	324.20 ± 10.24	0.60 ± 2.93	88.64	43.33

2015) and the International Committee on Radiation Protection established the risk conversion factor to be 0.05 Sv^{-1}. The global average is 0.29×10^{-3} and the maximum acceptable limit is 10^{-3} (UNSCEAR, 2000).

$$ELCR = AED_{outdoor} \times LE \times RF \qquad (11)$$

3 Results

The specific activities of Ra-226, Th-232, K-40 and Cs-137 radioactive nuclei was measured in 30 soil samples. The data results are listed in Table 1. Based on the data from Table 1, the highest value of the specific activity of Ra-226 was obtained in sample S7, and the lowest in sample S10. The highest and lowest value of specific activity of Th-232 radioactive nucleus is in samples S2 and S13, respectively. The highest value of the specific activity of the K-40 nucleus was obtained in sample S27 and the lowest amount of activity was obtained in sample S16. The Cs-137 with a maximum value of 4.45 Bq.kg^{-1} was measured in Samples S1, S16, S24, S25, S26, and S27, and for the rest of the samples was lower than the MDA level of the detector system. The calculated radiological parameters are presented in Table 2. The values of radiological risk parameters such as Ra_{eq}, AED_{out}, AED_{int}, D, H_{ex}, H_{in}, and I_{γ} varied in the range of 52.02 to 139.54) Bq.kg^{-1}, 24.98 to 68.27 and 122.57 to 334.93 in μSv.y^{-1}, 42.90 to 117.22 nGy.h^{-1}, 0.14 to 0.37, 0.16 to 0.40, 0.27 to 1.04, respectively. Figure 3 shows the comparison of the equivalent activity value of radium in this study with other countries. According to this figure, Pakistan shows a higher equivalent activity value compared to other countries. On the other hand, all values are lower than the global average value.

Figure 4 compares the gamma index value in this study with other countries where Turkey and Pakistan show the highest and the lowest gamma index values, respectively, compared to other countries. For all mentioned countries except Turkey, the gamma index values were lower than the global average. The range of ELCR values for soil samples ranged from 0.15×10^{-3} to 0.41×10^{-3}, which for samples s4, s14, s24, s27, s28, s29, and s30 was greater than the global average of 0.29×10^{-3}. Maps of Ra-226 distribution and airborne dose rate by GIS software are shown in Figs. 5 and 6. Ra-226 was higher at several locations near the central part of the city, and the absorbed

Table 2: Radiological parameters of samples.

Sample code	Radiological Index					
	AED_{out} (μSv.y^{-1})	AED_{in} (μSv.y^{-1})	H_{ex}	H_{in}	I_{γ}	$ELCR$ ($\times 10^{-3}$)
S1	66.05	188.48	0.21	0.25	0.59	0.23
S2	111.79	319.42	0.36	0.39	0.98	0.39
S3	81.16	231.88	0.25	0.27	0.72	0.28
S4	89.93	256.95	0.28	0.30	0.80	0.31
S5	61.25	175.02	0.19	0.32	0.54	0.21
S6	84.95	242.73	0.27	0.27	0.75	0.29
S7	72.51	207.18	0.23	0.32	0.64	0.25
S8	66.22	189.20	0.21	0.23	0.58	0.23
S9	63.87	182.49	0.20	0.20	0.56	0.23
S10	67.11	191.75	0.21	0.21	0.59	0.23
S11	50.16	143.33	0.15	0.16	0.44	0.17
S12	83.47	238.51	0.26	0.26	0.74	0.29
S13	55.94	159.83	0.18	0.25	0.50	0.19
S14	91.10	260.300	0.28	0.31	0.81	0.31
S15	60.27	172.22	0.19	0.20	0.53	0.21
S16	53.86	153.89	0.18	0.26	0.63	0.18
S17	63.76	182.18	0.20	0.22	0.39	0.22
S18	63.95	182.73	0.20	0.22	0.56	0.22
S19	64.53	184.39	0.20	0.22	0.57	0.22
S20	52.24	149.27	0.17	0.20	0.46	0.18
S21	42.90	122.57	0.14	0.17	0.38	0.15
S22	47.66	136.18	0.15	0.19	0.42	0.16
S23	74.68	213.37	0.24	0.30	0.66	0.26
S24	89.97	257.05	0.14	0.32	0.80	0.31
S25	74.67	213.37	0.23	0.25	0.66	0.26
S26	82.76	236.62	0.26	0.28	0.74	0.28
S27	98.22	280.64	0.31	0.32	0.27	0.34
S28	105.34	300.99	0.33	0.36	0.93	0.36
S29	117.22	334.93	0.37	0.40	1.04	0.41
S30	94.65	270.43	0.30	0.32	0.84	0.33
MIN	42.90	122.57	0.14	0.16	0.27	0.15
MAX	117.22	334.93	0.37	0.40	1.04	0.41
MEAN	74.40	212.59	0.22	0.26	0.63	0.25

Table 3: Comparison of specific activity and risk indicators with other countries of the world.

Country	Specific Activity			Radiological Index			Reference
	Ra-226	Th-232	K-40	Ra_{eq}	I_{γ}	H_{ex}	
Nigeria	18.00	22.00	210.00	65.63	0.21	0.18	(Agbalagba and Onoja, 2011)
Najaf	5.50	9.05	332.92	44.08	0.13	0.09	(Hussain and Alzhraa, 2017)
Nigeria(Ogun)	25.49	64.89	181.38	134.97	0.07	0.36	(Adewoyin et al., 2022)
Iraq	58.80	42.38	1025.35	198.37	0.73	0.53	(Hasan and Majeed, 2013)
Turkey	85.75	51.08	771.57	85.75	1.60	0.59	(Dizman et al., 2016)
Saudi	23.2	7.73	278.00	23.19	0.45	0.15	(Alshahri and El-Taher, 2019)
Pakistan	69.50	123.68	453.60	281.27	0.14	0.75	(Khan et al., 2020)
India	36.12	50.45	315.35	130.33	0.48	0.36	(Suresh et al., 2020)
Congo	25.14	18.16	46.15	64.70	0.44	0.17	(Diahou et al., 2022)
China	38.00	57.60	838.00	184.89	0.62	0.50	(Ziqiang et al., 1988)
Egypt	12.88	12.33	445.33	66.36	0.24	0.04	(El-Araby et al., 2021)
Malaysia	37.00	53.00	293.00	135.35	0.43	0.37	(Alzubaidi et al., 2016)
Iran (Sareband)	37.27	43.18	604.05	148.91	0.49	0.39	(Pourimani et al., 2017)
Iran (Shazand)	23.99	31.74	461.09	108.08	0.73	0.29	(Mohebian and Pourimani, 2020)
Iran	10.99	35.36	324.20	88.64	0.63	0.22	Present study

dose rate was higher in the southeastern part of the city. The Borujerd is a mountain city where the kind stones are igneous and sedimentary that causing in some regions the radioactivity to increase or decrease. This study showed that, in general, the amount of radiation and the doses absorbed was lower than the global average and do not pose a threat to human health.

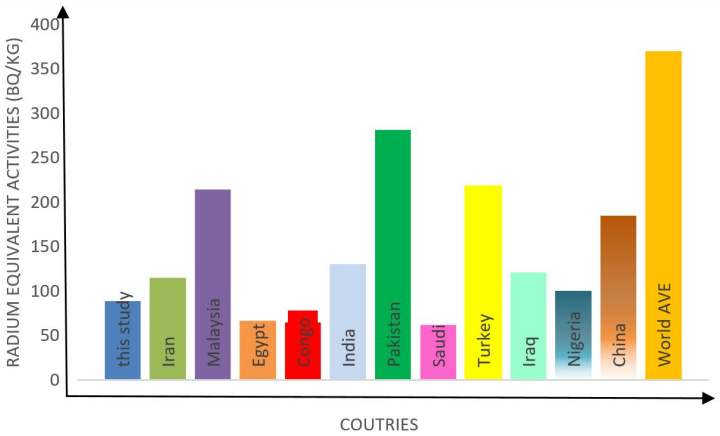

Figure 3: Comparison of the radium equivalent activity value of this study with other countries.

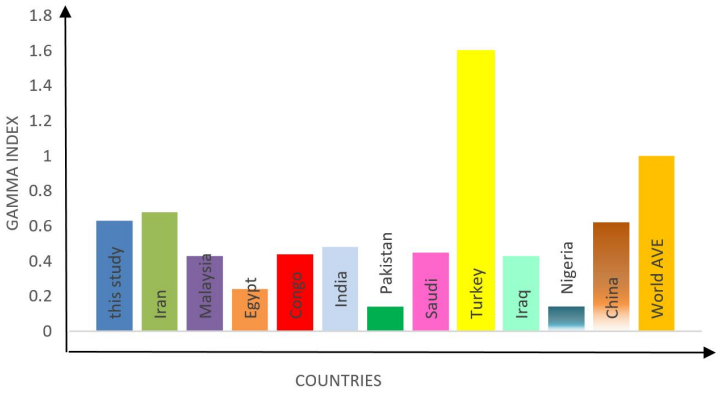

Figure 4: Comparing the gamma index of this study with other countries.

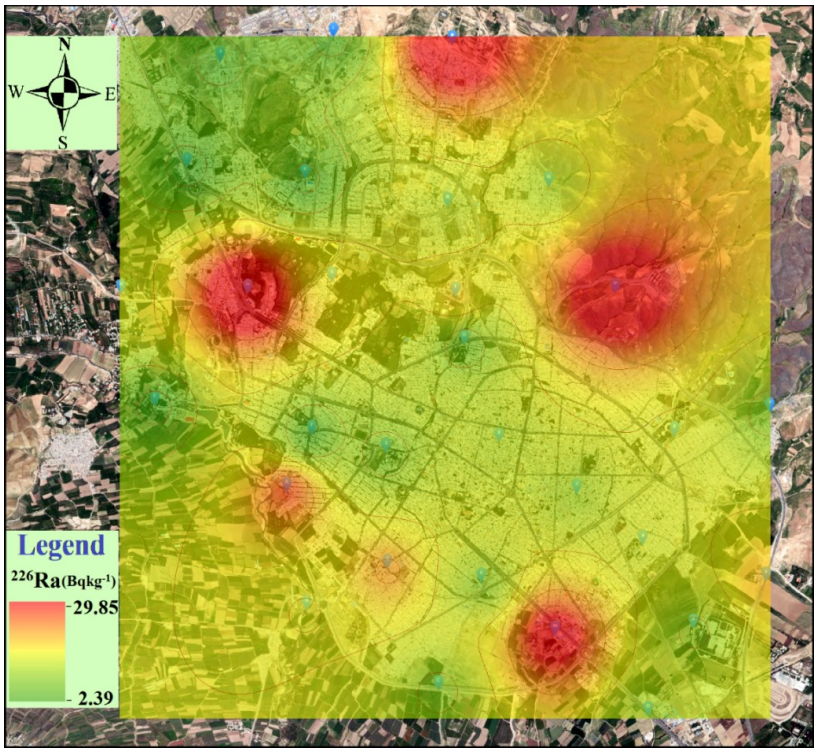

Figure 5: Radium distribution in Borujerd city in Iran.

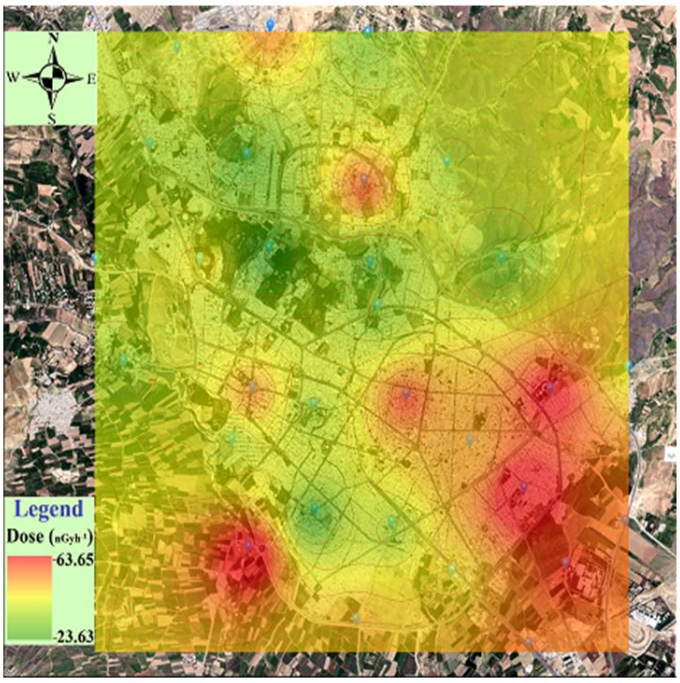

Figure 6: Dose map assignment of Borujerd City in Iran.

4 Conclusions

The study examined the radioactivity of soil samples in the city of Borujerd. The amount of natural radioactive elements was below the global average, and cesium was not detectable in most samples. Radiological parameters of soil samples were calculated and maps of radium distribution and absorbed dose in the air were drawn with the use of GPS software. The quantities of radiological parameters were lower than the global values, and in this sense, the existing nuclear radiation does not pose a threat to the city's inhabitants.

Acknowledgment

This work was funded by the Research Council of Arak University, so the authors of this article are grateful.

Conflict of Interest

The authors declare no potential conflict of interest regarding the publication of this work.

References

Adewoyin, O., Maxwell, O., Akinwumi, S., et al. (2022). Estimation of activity concentrations of radionuclides and their hazard indices in coastal plain sand region of Ogun state. *Scientific Reports*, 12(1):1–8.

Agbalagba, E. and Onoja, R. (2011). Evaluation of natural radioactivity in soil, sediment and water samples of Niger Delta (Biseni) flood plain lakes, Nigeria. *Journal of Environmental Radioactivity*, 102(7):667–671.

Alshahri, F. and El-Taher, A. (2019). Investigation of Natural Radioactivity Levels and Evaluation of Radiation Hazards in Residential-Area Soil Near a Ras Tanura efinery, Saudi Arbia. *Polish Journal of Environmental Studies*, 28(1).

Alzubaidi, G., Hamid, F., and Abdul Rahman, I. (2016). Assessment of natural radioactivity levels and radiation hazards in agricultural and virgin soil in the state of Kedah, North of Malaysia. *The Scientific World Journal*, 2016.

Annex, D., on the Effects of Atomic Radiation, U. N. S. C., et al. (2000). Sources and effects of ionizing radiation. *Investigation of I*, 125.

Barnett, C., Belli, M., Beresford, N., et al. (2009). *Quantification of Radionuclide Transfer in Terrestrial and Freshwater Environments for Radiological Assessments. IAEA-TECDOC-1616*. IAEA.

ÇINAR, H. and Altundaş, S. (2015). A Preliminary Indoor Gamma-ray Measurements in Some of the Buildings at Karadeniz Technical University (Trabzon, Turkey) Campus area. *Eastern Anatolian Journal of Science*, 1(1):10–19.

Diahou, R. R. C. M., Bounouira, H., Dallou, G. B., et al. (2022). Environmental radioactivity measurement in soils of an abandoned potash deposit at Holle, Republic of Congo. In *E3S Web of Conferences*, volume 336, page 00030. EDP Sciences.

Dizman, S., Görür, F. K., and Keser, R. (2016). Determination of radioactivity levels of soil samples and the excess of lifetime cancer risk in Rize province, Turkey. *International Journal of Radiation Research*, 14(3):237.

El-Araby, E., Shabaan, D., and Yousef, Z. (2021). Evaluation of radon concentration and natural radioactivity exposure from the soil of Wadi Hodein region, Egypt. *International Journal of Radiation Research*, 19(3):719–727.

Hasan, A. K. and Majeed, H. N. (2013). Natural radioactivity measurement in soil samples from the new Kufa University location, Iraq. *Journal: Journal of Advances in Physics*, 3(2).

Hossain, M. K., Hossain, S. M., Azim, R., et al. (2010). Assessment of radiological contamination of soils due to shipbreaking using HPGe digital gamma-ray spectrometry system. *Journal of Environmental Protection*, 1(1):10.

Hussain, H. H. and Alzhraa, W. S. A. (2017). Natural radioactivity levels of agricultural and virgin clay soil samples at al Najaf governorate. *American Journal of Research*, pages 3–15.

Jibiri, N. and Esen, N. (2011). Radionuclide contents and radiological risk to the population due to raw minerals and soil samples from the mining sites of quality ceramic and pottery industries in Akwa Ibom, Nigeria. *Radioprotection*, 46(1):75–87.

Kabir, K., Islam, S., and Rahman, M. (2009). Distribution of radionuclides in surface soil and bottom sediment in the district of Jessore, Bangladesh and evaluation of radiation hazard. *Journal of Bangladesh Academy of Sciences*, 33(1):117–130.

Khan, I., Qin, Z., Xie, T., et al. (2020). Evaluation of health hazards from radionuclides in soil and rocks of North Waziristan, Pakistan. *International Journal of Radiation Research*, 18(2):243–253.

Mohebian, M. and Pourimani, R. (2019). Measurement of radioactivity levels and health risks in the surrounding soil of shazand refinery complex in Arak, Iran, using gamma-ray spectrometry method. *Iranian Journal of Medical Physics*, 16(3):210–216.

Mohebian, M. and Pourimani, R. (2020). Radiometric properties of virgin and cultivated soil around the Shazand Refinery Complex in Iran. *International Journal of Radiation Research*, 18(4):723–732.

Pourimani, R. and Davood Maghami, T. (2020). Measurement of Radioactivity of Surface Soil in the East of Shazand Power Plant. *Journal of Environmental Science and Technology*, 22(4):109–119.

Pourimani, R. and Mohebian, M. (2021). Study of Background Correction of Gamma-Ray Spectrometry Using Reference Materials. *Iranian Journal of Science and Technology, Transactions A: Science*, 45(2):733–736.

Pourimani, R., Yousefi, F., et al. (2017). Investigation of natural radioactivity of agricultural and virgin soils in Arak and Saraband cities in Markazi province, Iran. *Journal of Water and Soil*, 31(5).

Ranjbar, H. and Yousefi, A. (2019). Identification and determination sources of uncertainty in measurement of activity in soil matrix. *Journal Modern Research Physics*, 4(1):19–28.

Suresh, S., Rangaswamy, D., Srinivasa, E., et al. (2020). Measurement of radon concentration in drinking water and natural radioactivity in soil and their radiological hazards. *Journal of Radiation Research and Applied Sciences*, 13(1):12–26.

UNSCEAR, U. (2000). Sources and effects of ionizing radiation. *United Nations Scientific Committee on the Effects of Atomic Radiation*.

Ziqiang, P., Yin, Y., and Mingqiang, G. (1988). Natural radiation and radioactivity in China. *Radiation Protection Dosimetry*, 24(1-4):29–38.

To cite this article:

Pourimani, R., Bajelan, M., Mohebian, M. (2023). Assignment of a radiological map of the city of Borujerd in Iran. *Radiation Physics and Engineering*, 4(2), 53-60.

DOI: 10.22034/rpe.2022.370078.1108

To link to this article: https://doi.org/10.22034/rpe.2022.370078.1108